Searching for Non-Gaussianities in the CMB

Martin Bucher, APC, Université Paris 7
Benasque, Spain, 2 August 2010

(with Bartjan Van Tent and Carla Sofia Carvalho), "Detecting Bispectral Acoustic Oscillations from Inflation Using a New Flexible Estimator," (astro-ph/0911.1642)

What is Non-Gaussianity ?

▶ Gaussian CMB Fluctuations

$$P(\{a_{\ell,m}\}) = \prod_{\ell,m}(2\pi)^{-1/2}\det{}^{-1/2}[C_\ell]$$
$$\times \exp\left[-\frac{1}{2}a_{\ell,m}^T C_\ell^{-1/2} a_{\ell,m}\right]$$

where

$$a_{\ell,m} = \begin{pmatrix} a_{\ell,m}^T \\ a_{\ell,m}^E \end{pmatrix}, \qquad C_\ell = \begin{pmatrix} C_\ell^{TT} & C_\ell^{TE} \\ C_\ell^{TE} & C_\ell^{EE} \end{pmatrix}$$

Happily most theories of inflation predict that the primordial cosmological perturbations should be Gaussian to a very high precision. Therefore after the data have beeen properly cleaned of all foreground and instrumental contamination, what is left should be perfectly Gaussian up to statistical noise.

▶ Non-Gaussian CMB fluctuations = Everything else

Problems in searching for non-Gaussianity

- Too many potential patterns of non-Gaussianity can be tested. Theoretical plausibility must be used in some way to limit the set of questions posed. 370 distinct questions neeed for 3σ result, 1.7 million for 5σ,....)

- Techniques used to process data (eg map making, foreground removal) are optimized for analyzing the Gaussian signal and consequently are susceptible to introduce spurious non-Gaussian signals.

Local type bispectral non-Gaussianity

Calculation of bispectrum predicted from single-field inflation (Maldacena, 2003 ; Acquaviva et al. 2003) has sparked an intense interested in non-Gaussianity from inflation.
The "local" ansatz

$$\Phi(\mathbf{x}) = \Phi_G(\mathbf{x}) + f_{NL} \left[\Phi_G{}^2(\mathbf{x}) - \langle \Phi_G{}^2(\mathbf{x}) \rangle \right],$$

is an reasonable (although not very good) approximation for single-field inflation and a better approximation for many multi-field models able to give bigger prediction for f_{NL}, although with new physics completely different shapes of bispectral anisotropy are possible as well.

f_{NL} from WMAP

- $-10 < f_{NL}^{local} < 74$(95% confidence) (Komatsu et al., WMAP 7-year official analysis)

- $27 < f_{NL}^{local} < 147$(95% confidence) (Yadav & Wandelt, independent analysis of WMAP 3-year maps)

- Many other independent analyses with broadly consistent but not identical conclusions

Defining the CMB bispectrum (without 3j symbols)

Triangle Inequality

L3

L1

L2

L1+L2+L3=0
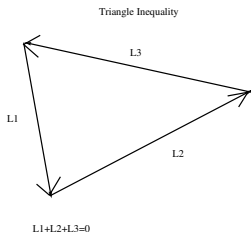
$$T(\Omega) = \sum_{\ell m} a_{\ell m} Y_{\ell m}(\Omega), \qquad a_{\ell m} = \int d\Omega \, Y_{\ell m}^*(\Omega) T(\Omega)$$

We define a family of maximally filtered maps

$$T_\ell(\widehat{\Omega}) = \sum_{m=-\ell}^{+\ell} a_{\ell m} Y_{\ell m}(\widehat{\Omega}).$$

and the "reduced bispectrum" is defined as

$$b_{\ell_1 \ell_2 \ell_3} = \int d\widehat{\Omega} \, T_{\ell_1}(\widehat{\Omega}) \, T_{\ell_2}(\widehat{\Omega}) \, T_{\ell_3}(\widehat{\Omega})$$

Intuitively the question is : does the product of two maps allow us the make any predictions regarding a third map ?

Bispectral estimators

We define the inner product on the space of possible bispectra

$$\langle b^A, b^B \rangle = \sum_{\ell_1 \leq \ell_2 \leq \ell_3} \frac{b^A_{\ell_1 \ell_2 \ell_3} b^B_{\ell_1 \ell_2 \ell_3}}{\text{Var}[b^{obs}_{\ell_1 \ell_2 \ell_3}]}$$

Here

$$\text{Var} \propto (c_{\ell_1} + n_{\ell_1})(c_{\ell_2} + n_{\ell_2})(c_{\ell_3} + n_{\ell_3})$$

Here n_ℓ is the noise from the experiment that dominates at large ℓ and serves as a cut-off.

$$\widehat{f}^{ideal}_{NL} = \frac{\langle b^{th}_{f_{NL}=1}, b^{obs} \rangle}{\langle b^{th}_{f_{NL}=1}, b^{th}_{f_{NL}=1} \rangle} = \sum_{\ell_1 \leq \ell_2 \leq \ell_3} w_{\ell_1 \ell_2 \ell_3} \frac{b^{obs}_{\ell_1 \ell_2 \ell_3}}{b^{th(f_{NL}=1)}_{\ell_1 \ell_2 \ell_3}},$$

Challenge is to weight the triplets so as to minimize the noise.

Qualitative nature of signal (I)

$$\Delta_\ell(k) \equiv \text{(CMB transfer function)}$$

[as computed by CMBFAST & CAMB for example]. Recall that the power spectrum is given by

$$c_\ell = \int_0^\infty dk\, P(k)\, |\Delta_\ell(k)|^2$$

and similarly the CMB bispectrum is given by

$$\mathfrak{b}_{\ell_1 \ell_2 \ell_3} = \int_0^\infty dk_1 \int_0^\infty dk_2 \int_0^\infty dk_3 \Delta_{\ell_1}(k_1)\Delta_{\ell_2}(k_2)\Delta_{\ell_3}(k_3)B_{3d}(k_1, k_2, k_3)$$

We may simplify (rather grossly) by assuming the Sachs-Wolfe formula

$$\frac{(\Delta T)}{T_0} \approx -\frac{1}{3}\Phi,$$

approximately valid for low-ℓ.

Qualitative nature of signal (II)

We obtain $\mathfrak{b}_{\ell_1 \ell_2 \ell_3} \sim \left(\ell_1^{-2}\ell_2^{-2} + \ell_2^{-2}\ell_3^{-2} + \ell_3^{-2}\ell_1^{-2} \right)$, giving a signal-to-noise squared

$$
\begin{aligned}
\left(\frac{S}{N} \right)^2 &\approx f_{NL}{}^2 \Omega_{sky} \int d^2\ell_1 \int d^2\ell_2 \int d^2\ell_3 \, \delta^2(\boldsymbol{\ell}_1 + \boldsymbol{\ell}_2 + \boldsymbol{\ell}_3). \\
&\times \frac{\left(\ell_1^{-2}\ell_2^{-2} + \ell_2^{-2}\ell_3^{-2} + \ell_3^{-2}\ell_1^{-2} \right)^2}{\ell_1^{-2}\ell_2^{-2}\ell_3^{-2}} \approx f_{NL}{}^2 \Omega_{sky} \frac{\ell^2 \ell^6}{\ell^8}
\end{aligned}
$$

By naive power counting, $(S/N)^2 \approx \Omega_{sky}\ell_{max}^2$, but a better approximatio is

$$
\left(\frac{S}{N} \right)^2 \approx f_{NL}{}^2 \Omega_{sky} \int d^2\ell_{big} \int \frac{d^2\ell_{small}}{\ell_{small}^2} \approx f_{NL}{}^2 \Omega_{sky}\ell_{max}^2 \ln \left(\frac{\ell_{max}}{\ell_{min}} \right)^2
$$

Komatsu, Spergel, Wandelt (2005) Estimator

An efficient implementation of the inverse variance weighted linear bispectral estimator :

$$S = 4\pi \int r^2 dr \int d\widehat{\Omega} \, A(r,\widehat{\Omega}) B^2(r,\widehat{\Omega})$$

where $A(r,\widehat{\Omega})$ is the CMB transfer function and $B(r,\widehat{\Omega})$ is the Wiener filter estimator for the primordial gauge-invariant potential Φ.

Improvements for cut-sky and non-uniform instrument noise due to Creminelli, Smith & Zaldarriaga.

Evaluation of the performance of non-ideal estimators

$$\widehat{f}_{NL}^{non-ideal} = \frac{\langle b^{templ}, b^{obs} \rangle}{\langle b^{templ}, b^{th}_{f_{NL}=1} \rangle}$$

$$\frac{\mathrm{Var}(\widehat{f}_{NL}^{non-ideal})}{\mathrm{Var}(\widehat{f}_{NL}^{ideal})} = \frac{\langle b^{th}_{f_{NL}=1}, b^{th}_{f_{NL}=1} \rangle}{\langle b^{templ}, b^{th}_{f_{NL}=1} \rangle} = \frac{1}{\cos^2 \theta}$$

There is an abundant literature emphasizing "optimal estimators", but it is a dangerous business to rely on a single number without asking more questions and trying to explain the result away.

Performance of binned bispectral estimator

Number bins	Overlap ($\cos^2 \theta$)
4	0.608
8	0.846
16	0.925
32	0.974
64	0.993

TAB.: Quality of estimator as a function of number of bins for $\ell_{max} = 2000$.

Dealing with bispectral contaminants

$b^{obs} = f_{NL}b^{th} + b^{cont} + b^{noise}$ where the three subscripts ℓ_1, ℓ_2, ℓ_3 are implied. We characterize the contaminant so that

$$\langle b^{cont} \rangle = 0, \quad C^{cont}_{\ell_1 \ell_2 \ell_3; \ell_1' \ell_2' \ell_3'} = \langle b^{cont}_{\ell_1 \ell_2 \ell_3} b^{cont}_{\ell_1' \ell_2' \ell_3'} \rangle$$

$$
\begin{aligned}
\mathcal{L} \quad \propto \quad & \int (\mathcal{D}b^{cont}) \exp\left[-\frac{1}{2} b^{cont\,T}(C^{cont})^{-1} b^{cont} \right] \\
& \times \exp\left[-\frac{1}{2}(b^{obs} - b^{cont} - f_{NL}b^{th})^T \times (C^G)^{-1}(b^{obs} - b^{cont} - f_{NL}b^{th}) \right],
\end{aligned}
$$

which may be evaluated to (up to an irrelevant factor)

$$\exp\left[-\frac{1}{2}(b^{obs} - f_{NL}b^{th})^T(C^G + C^{cont})^{-1}(b^{obs} - f_{NL}b^{th}) \right] \propto \exp\left[-\frac{1}{2}\frac{(f_{NL} - \widehat{f}_{NL}^{ml})^2}{\sigma_{f_{NL}}^2} \right].$$

$$\widehat{f}_{NL}^{ml} = \frac{b^{th\,T}(C^G + C^{cont})^{-1} b^{obs}}{b^{th\,T}(C^G + C^{cont})^{-1} b^{th}},$$

and the "information" is given by

$$\frac{1}{\sigma_{f_{NL}}^2} = b^{th\,T}(C^G + C^{cont})^{-1} b^{th}.$$

Plotting the predicted bispectrum
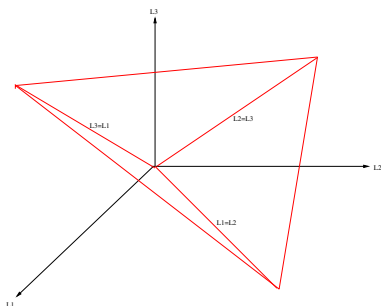
Approximations to the bispectrum :

$$\mathcal{B}_{approx,I} \propto \ell_1^{-2}\ell_2^{-2} + \ell_2^{-2}\ell_3^{-2} + \ell_2^{-2}\ell_1^{-2}$$

$$\mathcal{B}_{approx,II} \propto c_{\ell_1}c_{\ell_3} + c_{\ell_2}c_{\ell_1} + c_{\ell_3}c_{\ell_2}$$

Quantities to plot (for $f_{NL} = 1$) :

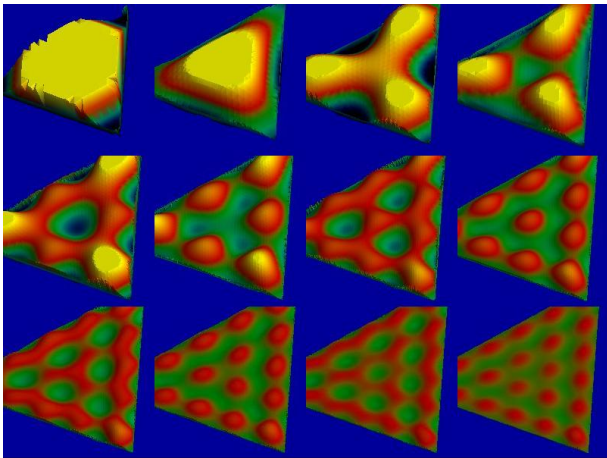$$\mathcal{B}_I = \mathcal{B}/\mathcal{B}_{approx,I}, \qquad \mathcal{B}_{II} = \mathcal{B}/\mathcal{B}_{approx,II}$$

FIG.: We plot the reduced CMB TTT bispectrum rendered dimensionless in a scale-free way according to the function $\mathcal{B}_{\ell_1 \ell_2 \ell_3}$ on 12 sections of constant $(\ell_1 + \ell_2 + \ell_3)/3$ corresponding to 200, 300, 400, 500, 600, 700, 800, 900, 1000, 1100, 1200, 1300. The color scale (explained in the text) ranges from -14.0 to $+14.0$ and values outside of this range are clipped.
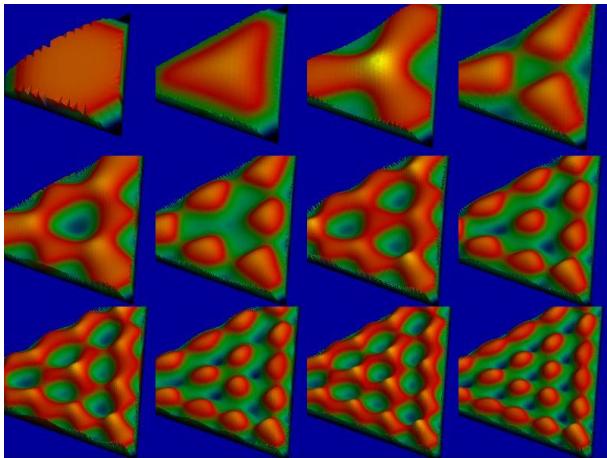
FIG.: Same as in Fig. 1 except that we instead plot $\bar{\mathcal{B}}_{\ell_1\ell_2\ell_3}$, normalized with the actual CMB temperature power spectrum rather than the scale free one. Here the color scale (same as above) ranges from -3.0 to $+3.0$.
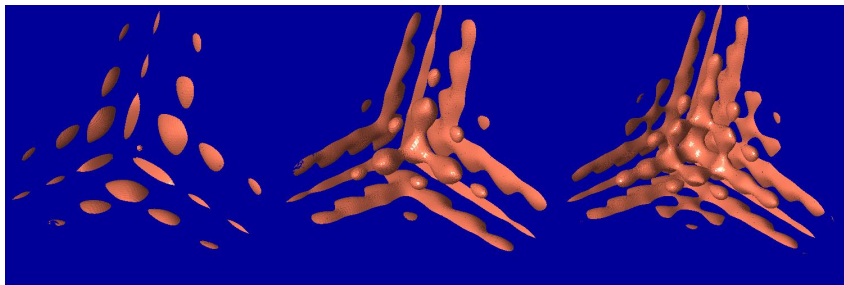
FIG.: A sequence of isosurfaces for the function $\mathcal{B}_{\ell_1\ell_2\ell_3}$ is shown for $\mathcal{B}$ = -10, -4, -2. [Additional and higher resolution isosurfaces may be found at the website indicated in the text.]
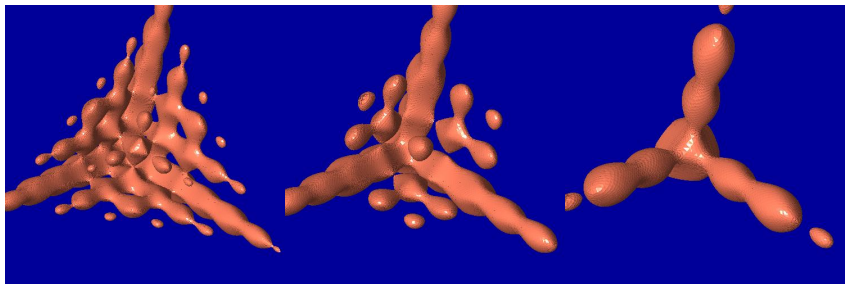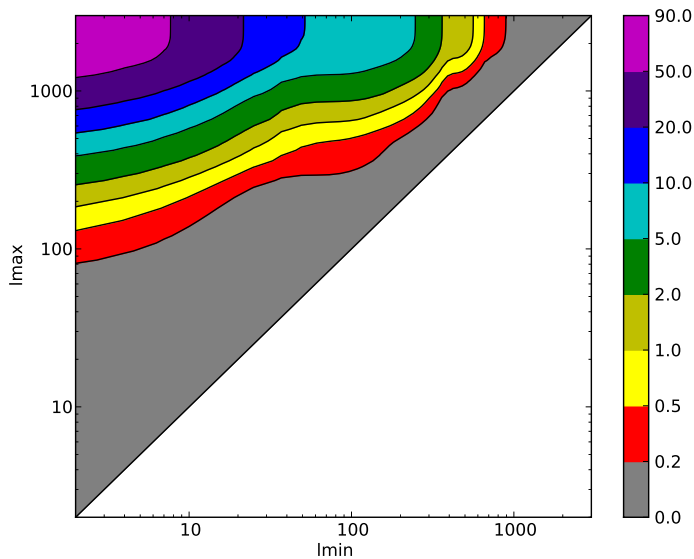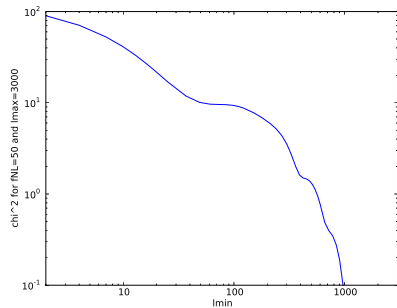
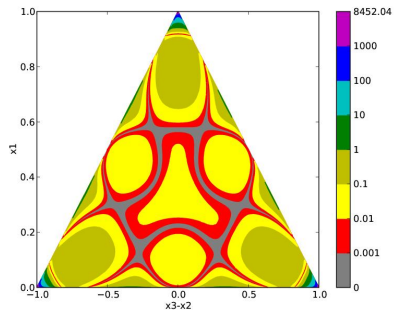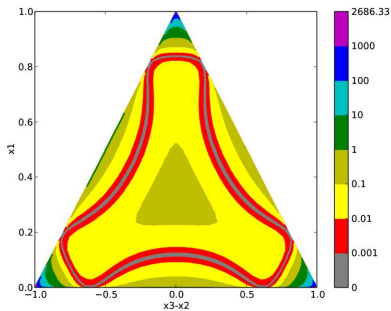FIG.: Continuation of previous figure, with isosurfaces at $\mathcal{B} = 2$, 4, and 10.

Where does the information lie ?
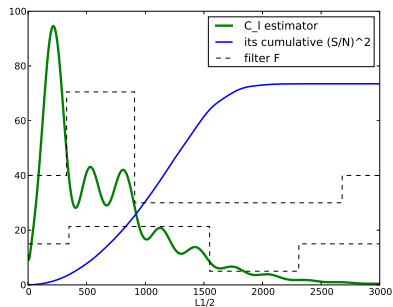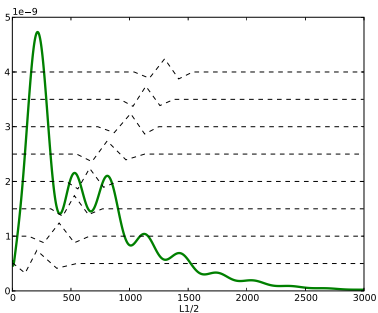
Decrease in χ^2 as ℓ_{min} is raised

Information as a function of triangle shape

Seeing the acoustic oscillations in the 3-point function

Detectibility of the various features

Feature	Center	$(\Delta\ell)_{left}$	$(\Delta\ell)_{right}$	$(S/N)^2$
1st peak	210	100	170	0.43
1st trough	400	130	130	0.69
2nd peak	530	100	120	0.19
2nd trough	660	100	120	0.27
3rd peak	810	130	160	0.70
3rd trough	1010	140	120	1.08
4th peak	1140	110	120	0.34
4th trough	1300	130	120	0.53
Drop A	910	580	1770	11.3
Drop B	1550	1200	760	21.9

assuming $f_{NL} = 50$
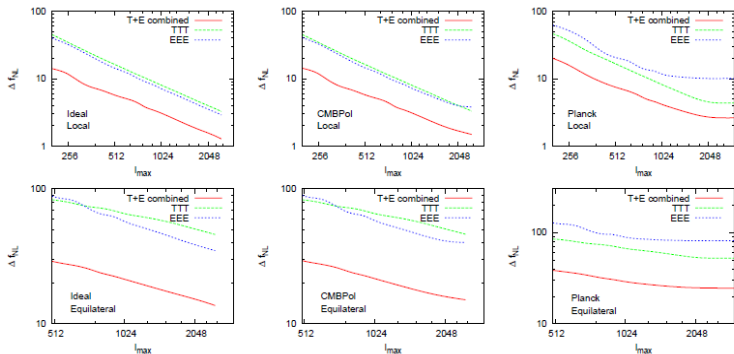
Future prospects :

FIG. 7: Fisher predictions for minimum detectable f_{NL} (at 1 σ) as a function of maximum multipole ℓ_{max}. Upper panels are for the local model while lower panels are for the equilateral model. Left panels shows an ideal experiment, middle panels are for CMBPol like experiment with noise sensitivity $\Delta_p = 1.4\mu$K-arcmin and beam FWHM $\sigma = 4'$ and right panels are for Planck like satellite with and noise sensitivity $\Delta_p = 40\mu$K-arcmin and beam FWHM $\sigma = 5'$. In all the panels, the solid lines represent temperature and polarization combined analysis; dashed lines represent temperature only analysis; dot-dashed lines represent polarization only analysis.

From Yadav & Wandelt, 2010

$$\left(\frac{S}{N}\right)^2 \approx f_{NL}{}^2 \Omega_{sky} \int d^2\ell_{big} \int \frac{d^2\ell_{small}}{\ell_{small}^2} \approx f_{NL}{}^2 \Omega_{sky} \ell_{max}^2 \ln\left(\frac{\ell_{max}}{\ell_{min}}\right)^2$$

Conclusions

- Searching for non-zero f_{NL}^{local} (and also other patterns of primordial bispectral non-Gaussianity) offers an exciting test of inflation and new revealing clues concerning the nature of the primordial perturbations.

- If a statistically significant signal is in fact found, we will want to divide the data and test the shape. The acoustic oscillations suggest one way to do this.

- f_{NL} searches in the CMB are largely limited by cosmic variance. We can do better than Planck with full-sky surveys at higher resolution and including by probing polarization at the highest ℓ, but the damping tail and predominance of non-primordial components at very large ℓ (esp., SZ and point sources) set a limit to how much improvement can be anticipated.